29th International Cosmic Ray Conference Pune (2005) **2**, 5–8

Anomalous and galactic cosmic ray He spectra near the termination shock

R.A. Caballero-Lopez[a,c] H. Moraal[b,c] and F.B. McDonald[c]
(a) Instituto de Geofísica, UNAM, 04510, México
(b) School of Physics, North-West University, Potchefstroom 2520, South Africa
(c) Institute for Physical Science and Technology, University of Maryland, College Park, MD, 20742, USA
Presenter: R.A. Caballero-Lopez (rogelioc@geofisica.unam.mx), mex-caballero-lopez-RA-abs1-sh31-oral

The third interaction of Voyager 1 with the termination shock in December 2004 was a crossing into the heliosheath that has produced cosmic ray intensity spectra from this region for the first time. In this paper we interpret these spectra in terms of standard modulation theory. We concentrate on He, which has both a well-defined anomalous and galactic component.

1. Introduction

Voyager 1 made two interactions with the solar wind termination shock in 2002/03 and 2003/04 (e.g. [1], [2] and [3]). The consensus is that during these events it did not actually cross the shock. On 16 December 2004, however, a third interaction was seen, and since the heliospheric magnetic field (HMF) made a significant and sustained jump (L.F. Burlaga, private communication), this has been interpreted as the shock crossing.

In this paper we interpret anomalous cosmic ray (ACR) He^{+} and galactic cosmic ray (GCR) He^{++} spectra from 12 to 19 June 2005, when Voyager 1 was inside the heliosheath. Figure 1A shows two of these spectra, being weekly averages for the periods 16-23 January and 12-19 June 2005. Data above the vertical line at 100 MeV/n are GCR He^{++}. Below this line the assumed ACR He^{+} spectrum is not immediately clear. At first, such as in the 16-23 January period, this spectrum did not unfold into the power law expected from shock acceleration. This unfolding only happened gradually, as shown by the filled symbols for 12-19 June.

This unfolding is not yet complete, because the 12-19 June data still has a feature at $T \approx 10$ MeV/n, marked by the second vertical line. This feature was very distinct in the 16-23 January period, and its origin is uncertain. The C to O ratio (M.E. Hill, private communication) indicates that the composition is typical of the ACR component down to at least 0.8 MeV/n O^{+}. The equivalent He^{+} energy is 3.2 MeV/n, so that all the data below 100 MeV/n in Figure 1A are probably ACR He^{+}. Figure 1B repeats the 12-19 June data, but shown together with that of Voyager 2 at 75 AU, well inside the shock, and also IMP8 at 1 AU for the period 13 October to 30 December 2004, before the large event of 20 January 2005, that has not reached the Voyagers yet, went through. The 10 to 100 MeV/n Voyager 2 data look like modulated intensities of the shock spectra. However, the Voyager 2 spectra below 10 MeV/n are similar to the Voyager 1 spectra, and therefore do not seem like a modulated shock spectrum. Due to its uncertain origin, we will not include this $T < 10$ MeV/n component in our fits of these observations.

The Voyager 2 ACR intensity maximum occurs at 35 MeV/n. During the previous two solar minima, these peaks occurred at $\approx$ 20 MeV/n in 1987 (when the Voyagers and Pioneer 10 were at 24, 33 and 42 AU), and at $\approx$ 6 MeV/n in 1997 (when they were between 52 and 66 AU). Presently the heliosphere is in the same qA$<$0 drift state as in 1987, while 1997 was a qA$>$0 period. The shift in peak energy from one solar minimum to the next is suggestive of drift effects, and it indicates that the current 35 MeV/n peak may unfold nearer to the 20 MeV/n value seen in 1987, than to the much lower value observed in 1997. We note, however, that [4] and [5] were unsuccessful to explain this shift in peak intensities in standard models of the modulation.

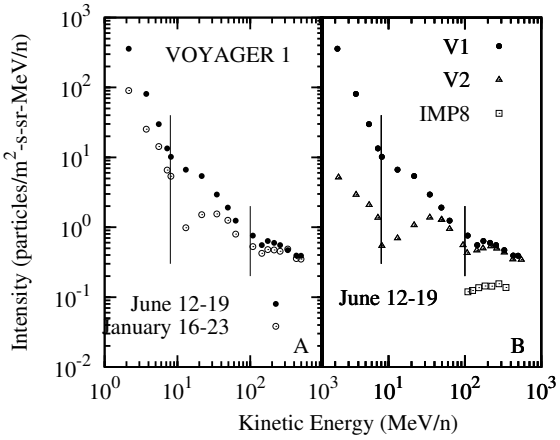

Figure 1. Panel A shows two weekly Voyager 1 spectra in January and June 2005. Panel B shows the Voyager 1 and Voyager 2 spectra for the last period, 12-19 June 2005, together with those of IMP8 at 1 AU. Vertical lines at 10 and 100 MeV/n demarcate different spectral features as described in the text.

2. Spectral Fits

Intensity spectra were calculated from numerical solutions of the cosmic ray transport equation for the evolution of the distribution function f in terms of particle momentum, p:

$$\frac{\partial f}{\partial t} + \mathbf{V}\cdot\nabla f - \nabla\cdot(\mathsf{K}\cdot\nabla f) - \frac{1}{3}(\nabla\cdot\mathbf{V})\frac{\partial f}{\partial \ln p} = Q. \quad (1)$$

Here $\mathbf{V}$ is the solar wind velocity and $\mathsf{K}(\mathbf{r},P,t)$ the diffusion tensor which contains elements $\kappa_{\parallel}(\mathbf{r},P,t)$ and $\kappa_{\perp}(\mathbf{r},P,t)$ for scattering along and perpendicular to the HMF, B, together with an antisymmetric coefficient $\kappa_T = \beta P/(3B)$ which describes gradient, curvature, neutral sheet, and shock drift effects . The HMF structure is described by the standard Parker spiral magnetic field, given in spherical polar coordinates (r,θ,ϕ) by $\mathbf{B} = B_e(r_e/r)^2(\mathbf{e}_r - \tan\psi\mathbf{e}_\phi)$, with $\tan\psi = \Omega(r-r_0)\sin\theta/V$, where Ω is the angular frequency of solar rotation, and r_0 is the Alfven radius of several solar radii. The values of the field at Earth, B_e, vary from 5 to 10 nT from solar minimum to maximum. The diffusion coefficients can be written in terms of mean free paths by $\kappa = 3\lambda/v$, and the radial and latitudinal components are $\lambda_{rr} = \lambda_{\parallel}\cos^2\psi + \lambda_{\perp}\sin^2\psi$, $\lambda_{\theta\theta} = \lambda_{\perp}$. Two sets of calculations were done. First, we used the simplest possible solution of the transport equation, the one-dimensional no-drift version, to demonstrate the main effects with the minimum number of parameters. The solution was then repeated for a full two-dimensional drift version of the equation in the qA<0 drift state with a wavy neutral sheet with a tilt angle of 30°.

One-dimensional Solution. A shock with compression ratio $s = 3$ was put at r_s = 90 AU and the outer boundary at r_b = 150 AU. The solar wind speed was V = 400 kms^{-1} inside the shock and $V = (400/s)(r_s/r)^2$ kms^{-1} in the heliosheath. The effective radial diffusion coefficient was $\kappa_{rr} = 3\text{x}10^{22}\beta P(\text{GV})$ cm^{2}s^{-1} inside the shock and $\kappa_{rr} = (3/s)\text{x}10^{22}\beta P(\text{GV})$ cm^{2}s^{-1} in the heliosheath. These parameters generate three numbers that determine the overall character of the solution. The first two are the values of the modulation integral

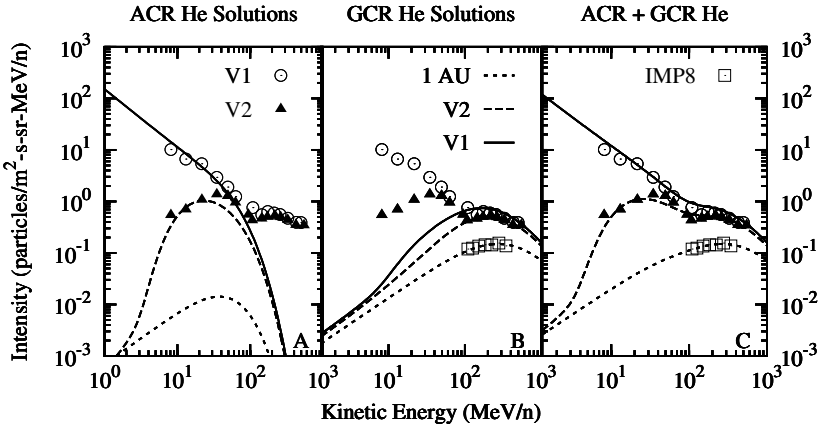

Figure 2. Solutions of the one-dimensional transport equation that fit the observations. The left hand panel shows ACR solutions, the middle one GCR solutions, and the right one the combined solutions. Parameters are described in the text.

$M = \int (V/\kappa_{rr})dr$ upstream of the shock in the supersonic wind and in the subsonic wind of the heliosheath. They are $M_{\rm upstream} = 1.8/(\beta P)$ and $M_{\rm downstream} = M_{\rm upstream}/3$, implying upstream and downstream Force-Field potentials of 600 MV and 200 MV. The third parameter is the cutoff energy for the acceleration where (see [6]) $V\,dr/\kappa_{rr} \approx 10$, only weakly dependent on s. For the present parameters this cutoff occurs at $\approx T = 40$ MeV/n.

The results are shown in Figure 2. From top to bottom, panel A shows the ACR He^+ solution at the positions of Voyager 1 at 96 AU, Voyager 2 at 70 AU, and IMP8 at 1 AU. The IMP 8 data are included to ensure that the correct amount of modulation throughout the entire heliosphere is reproduced. The middle panel shows the GCR He^{++} solution for the same positions, with a local interstellar input spectrum of the form $j_{Tb} = 1.075T^{-2.8}/(1 + 3.91T^{-1.09} + 0.9T^{-2.54})$ on the outer boundary at r_b, taken from [7]. Panel C is the combination of the previous two. This shows that the main features of these spectra can be represented satisfactory with this simple parameterization. The shock compression ratio s is not an important parameter, and almost similar solutions can be achieved for a stronger shock with $s = 4$.

qA<0 Drift Solution. At the present time the heliosphere is in the recovery phase of a qA<0 drift state in which positively charged particles drift inwards along the way neutral sheet, polewards from there, and from the pole to the ecliptic along the shock. At present the tilt angle of the sheet is between 30° and 40°. These drift effects influence the cosmic ray transport. Therefore, the calculations were repeated with a two-dimensional (radial distance, polar angle) solution, including these drifts, with the results shown in Figure 3. The values of r_s, r_b, V, and s are the same as in the one-dimensional case, with both V independent of polar angle. However, κ_{rr} in the ecliptic plane is 1.76 times larger than in one–dimensional case and dropping with a factor of 4 towards the poles. The latitudinal diffusion coefficient $\kappa_{\theta\theta}$ is 70% of κ_{rr} in the ecliptic, and is independent of position. The drift effect was scaled down by a factor from the normal full-drift effect experienced at solar minimum conditions. Thus, drift effects alter the modulation parameters moderately, but the basic explanation of the spectra remains the same.

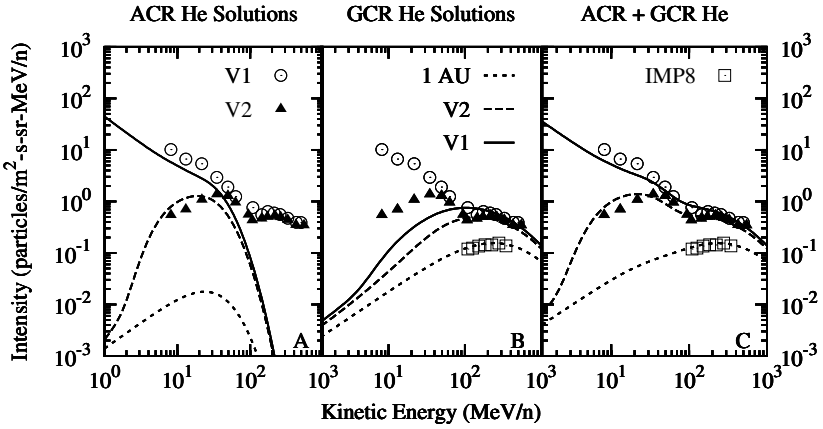

Figure 3. Solutions of the two-dimensional transport equation for the qA<0 drift state in the same format as Figure 2. Parameters are described in the text.

3. Conclusions

The most recent spectra observed by Voyager 1 in the heliosheath beyond the solar wind termination shock can be explained in a standard model of heliospheric modulation and acceleration on the shock. The main features can be understood in terms of the modulation integrals inside and outside the shock, and the cutoff energy, all of which are determined by the solar wind speed and the effective radial diffusion coefficient. These parameters vary moderately in a more realistic two-dimensional drift model with a wavy neutral sheet in the current qA<0 drift state of the heliosphere.

Acknowledgements. This work was supported by NSF Grant ATM 0107181 and the South African National Research Foundation. RCL was supported by UNAM-DGAPA grant IN106105.

References

[1] S.M. Krimigis et al., Nature, 425, 46, (2003).
[2] F.B. McDonald et al., Nature, 426, 48, (2003).
[3] F.B. McDonald et al., AIP Conf. Proc., 719, 139, (2004).
[4] C.D. Steenberg, Ph.D. thesis, Potchefstroom University, (1998).
[5] J.P.L. Reinecke et al., J. G. R., 105, 27439, (2000).
[6] C.D. Steenberg and H. Moraal, J. G. R., 104, 24879, (1999).
[7] R.A. Caballero-Lopez et al., J.G.R., 109, A05105, doi:10.1029/2003JA010358, (2004).